-decay study of ^{182,184}Tl

2016 J. Phys. G: Nucl. Part. Phys. 43 025102

(http://iopscience.iop.org/0954-3899/43/2/025102)

IOP Publishing Journal of Physics G: Nuclear and Particle Physics

J. Phys. G: Nucl. Part. Phys. **43** (2016) 025102 (22pp) doi:10.1088/0954-3899/43/2/025102

α-decay study of ^{182,184}Tl

C Van Beveren[1], A N Andreyev[2,3], A E Barzakh[4], T E Cocolios[5,6], R P de Groote[1], D Fedorov[4], V N Fedosseev[7], R Ferrer[1], L Ghys[1,8], M Huyse[1], U Köster[9], J Lane[10], V Liberati[10], K M Lynch[5,6], B A Marsh[7], P L Molkanov[4], T J Procter[6], E Rapisarda[1,5], K Sandhu[10], M D Seliverstov[2,4,7,10], P Van Duppen[1], M Venhart[11] and M Veselský[11]

[1] KU Leuven, Instituut voor Kern- en Stralingsfysica, B-3001 Leuven, Belgium
[2] Department of Physics, University of York, YO10 5DD, UK
[3] Advanced Science Research Center (ASRC), Japan Atomic Energy Agency (JAEA), Tokai-mura, Naka-gun, Ibaraki, 319–1195, Japan
[4] Petersburg Nuclear Physics Institute, NRC Kurchatov Institute, 188300 Gatchina, Russia
[5] ISOLDE, CERN, CH-1211 Geneve 23, Switzerland
[6] The University of Manchester, School of Physics and Astronomy, Oxford Road, Manchester M13 9PL, UK
[7] EN Department, CERN, CH-1211 Geneve 23, Switzerland
[8] Belgian Nuclear Research Centre SCK • CEN, Boeretang 200, B-2400 Mol, Belgium
[9] Institut Laue Langevin, 6 rue Jules Horowitz, F-38042 Grenoble Cedex 9, France
[10] School of Engineering and Science, University of the West of Scotland, Paisley PA1 2BE, UK
[11] Institute of Physics, Slovak Academy of Sciences, 845 11 Bratislava, Slovakia

E-mail: celine.vanbeveren@fys.kuleuven.be

Received 11 September 2015
Accepted for publication 6 November 2015
Published 8 January 2016

Abstract

α-decay spectroscopy of ^{182,184}Tl has been performed at the CERN isotope separator on-line (ISOLDE) facility. New fine-structure α decays have been observed for both isotopes. α-decay branching ratios of 0.089(19)%, 0.047 (6)% and 1.22(30)% have been deduced for the (10^-), (7^+) and (2^-) states respectively in ^{184}Tl and a lower limit of 0.49% for the α-decay branching ratio of ^{182}Tl. A new half-life of 9.5(2) s for the (2^-) state in ^{184}Tl and 1.9(1) s for the low-spin state in ^{182}Tl has been deduced. Using α–γ coincidence analysis, multiple γ rays were observed de-exciting levels in ^{178,180}Au fed by ^{182,184}Tl α decays. The γ transitions connecting these low-lying states in ^{178,180}Au are essential to sort the data and possibly identify bands from in-beam studies in these isotopes. Owing to the complex fine-structure α decays and limited knowledge about the structure of the daughter nuclei, only partial

level schemes could be constructed for both gold isotopes in the present work. Reduced α-decay widths have been calculated and are compared with values obtained in neighboring odd-A and even-A thallium isotopes. Except for the allowed α decay of the ^{184}Tl (10^-) state, the other fine-structure α decays observed in this study are hindered. This points to strong structural changes between parent thallium and daughter gold isotopes.

Keywords: intruder states, shape coexistence, α-spectroscopy, isomerism

(Some figures may appear in colour only in the online journal)

1. Introduction

Although close to the $Z = 82$ shell closure, neutron-deficient nuclei with an odd number of protons and an odd number of neutrons (so called odd–odd nuclei) below lead exhibit complex structures even at low excitation energy. The coupling of an unpaired proton and unpaired neutron gives rise to multiplets of low-lying states from which some can be isomeric [1]. Furthermore this region is notorious for intruder states and shape coexistence [2]. This makes the decay and level schemes of odd–odd nuclei complicated and the spectroscopic interpretation of the underlying configurations of the observed states in many isotopes puzzling. The observation of hindered and unhindered α decay is a powerful method to selectively study and identify these low-lying states in the daughter nuclei, yielding direct information on the excitation energy, decay pattern and possible configurations involved (see e.g. [3–6] and references therein). In this paper we report on an α-decay study of ^{182,184}Tl ($Z = 81$) which is part of an experimental campaign dedicated to decay and laser spectroscopy studies of neutron-deficient thallium isotopes performed at the isotope separator on-line (ISOLDE) [7] CERN, Geneva, Switzerland.

Prior to our study, α decay was identified for ^{184}Tl [8] and two α lines of 5988(5) keV and 6162(5) keV were assigned to this isotope based on their similar deduced half-lives of 10 (2) s. The authors reported also a third less intense α line around 5815 keV that seemed to decay with a similar half-life. An α-decay branching ratio of 2.1(7)% was extracted using the intensities of both α lines and the intensity of the 367 keV $2^+ \rightarrow 0^+$ transition in ^{184}Hg, which was reported [9] to encompass 80(5)% of the EC/β^+ decay intensity. Alpha decay of ^{184}Tl was also observed by Schrewe *et al* [10]. Two α lines with energies 5983(10) and 6155(10) keV were observed, in agreement with those reported by [8], but the authors also identified an α line originating from ^{184}Tl at an energy of 6066(15) keV.

A β-decay study of ^{184}Tl yielded two β-decaying states, with proposed spin and parity (7^+) and (2^-) based on observed β feeding to the 8^+ as well as to the first excited 2^+ [9]. Both β decays exhibit a half life of 11(1)s [9]. In an α-decay study of ^{188}Bi [5] three long-living states have been identified in daughter ^{184}Tl. The (10^-) state in ^{188m1}Bi, of which the assumed major configuration is $[\pi 1h_{9/2} \otimes \nu 1i_{13/2}]$, decays via an unhindered α decay to a (10^-) state and strongly hindered to a (7^+) state in ^{184}Tl. The $(3^+)[\pi 1h_{9/2} \otimes \nu 3p_{3/2}\ ]$ state ^{188m2}Bi decays unhindered to a (3^+) state, explained as a $[\pi 1\, h_{9/2} \otimes \nu 3p_{3/2}\ ]$ intruder state, 99 keV above the weakly fed (2^-) state, explained as regular $[\pi 3\, s_{1/2} \otimes \nu 3p_{3/2}]$ state. As the relative position of the α-decaying states in ^{188}Bi is not known [5], the relative position of the (7^+) and (2^-) ^{184}Tl states are not determined. Direct mass measurements in a penning trap could not resolve this [11]. In our experimental campaign, an excitation energy of 506.1(1) keV, relative to the (7^+) state, and a half-life of 47.1(7) ms of the intruder-based (10^-) state in ^{184}Tl

have been determined [12]. A review of hindered and unhindered α-decay data of $^{187-192}$Bi populating levels in daughter nuclei $^{183-188}$Tl including the new information is given in [12] and supports the interpretation of the intruder character of the (10^-) state in ^{184}Tl.

The first identification of ^{182}Tl α decay was by Keller *et al* [13] at the velocity filter SHIP. The authors assigned a 6406(10) keV α line to ^{182}Tl based on excitation functions. No half-life information was deduced in this study. Bolshakov *et al* [14] reported on the observation of 6050 keV α particles from ^{182}Tl with a half-life of 2.8(6) s. The authors of [14–16] deduced an upper limit of 4%, 5% and 5% respectively for the α-branching ratio of ^{182}Tl.

Previous α-decay studies of two isomeric states in ^{186}Bi proposed the existence of two isomeric states in the daughter ^{182}Tl [6]. Similar to ^{184}Tl, the relative position of the α-decaying states in ^{186}Bi is not known, thus the relative position of the two isomeric states in ^{182}Tl is not fixed. Based on a change of decay pattern observed in the neighboring isotope ^{188}Bi, the authors did not suggest any tentative spin/parity assignments for ^{186}Bi and ^{182}Tl and stress that all possible proton–neutron combinations leading to states with the same spin and parity should be considered.

In the even mass $^{186-204}$Tl isotopes, both $[\pi 3s_{1/2} \otimes \nu 1i_{13/2}]_{7^+}$ and $[\pi 3s_{1/2} \otimes \nu 3p_{3/2}$ or $\pi 3s_{1/2} \otimes \nu 2f_{5/2}]_{2^-}$ configurations have been suggested for the β- and/or α-decaying ground and isomeric states. Only for $A = 190$ and $A \geqslant 194$ measurements have established $J = 2$ for the ground state spins [17–20]. For all lighter isotopes, assignments rely on assumptions based on extrapolations using systematics. For the even mass thallium isotopes with $A \geqslant 186$ $J^\pi = (2^-)$ and $J^\pi = (7^+)$ have been adopted for the ground state and the excited isomeric state respectively and this sequence is extrapolated down to ^{182}Tl on systematic grounds [21]. According to [15] a (7^+) assignment for the ^{182}Tl parent state with 3.1(10) s half-life is supported by the observed level population up to 8^+ in ^{182}Hg fed by ^{182}Tl β decay. When moving towards the lighter thallium isotopes with $N = 99$ and lower, a neutron configuration change to $[\pi 3s_{1/2} \otimes \nu 1h_{9/2}]_{4^-,5^-}$ is expected. This change was already demonstrated in the neighboring lead, mercury and platinum nuclei at neutron numbers below 100 by, e.g. α-decay studies of ^{179,181}Pb [22–24] or by observation of low-lying $9/2^-$ (or $7/2^-$ of $\nu 1h_{9/2}$ parentage) states in $N = 99$, 101 mercury and platinum [25]. Therefore a change of the $[\pi 3\, s_{1/2} \otimes \nu 1i_{13/2}]_{7^+}$ to $[\pi 3s_{1/2} \otimes \nu 1h_{9/2}]_{4^-,5^-}$ can be expected to occur around ^{180,182}Tl. The $[\pi 3\, s_{1/2} \otimes \nu 1\, h_{9/2}]_{4^-,5^-}$ configuration has been proposed by Elseviers *et al* [26] for the ground state of ^{180}Tl in a previous study at ISOLDE, CERN. The presence of the $[\pi 3\, s_{1/2} \otimes \nu 3p_{3/2}]_{2^-}$ can also not be excluded in ^{182}Tl since it has been established in the heavier odd–odd thallium isotopes. Besides these configurations based on the regular $\pi 3s_{1/2}$ orbital, neutrons in the $i_{13/2}$ and $h_{9/2}$ orbitals can also couple to the intruder $\pi h_{9/2}$ configuration. Similar states have been observed at relatively low excitation energy in odd–odd thallium isotopes with $A \geqslant 184$ and coexistence of all these, in some cases isomeric, states are thus not excluded in ^{182}Tl. The laser spectroscopy measurements from the present campaign confirm the presence of two long-living states in ^{182}Tl [27] as deduced from differences in the hyperfine structure patterns in both α- and γ-decay data.

Combining the high selectivity of the resonant ionization laser ion source (RILIS) [28–30] with decay spectroscopy and the in-source laser spectroscopy method [31–33], exotic thallium isotopes down to $N = 97$ have been studied at the ISOLDE facility using the Windmill detection system [34–36]. Complementary decay data on isomerically purified sources were collected. In the present study, the α-decay characteristics of ^{182,184}Tl are reported. The results on the β decay of ^{182,184}Tl will be reported elsewhere [37].

2. Experimental setup

The ^{182}Tl and ^{184}Tl α-decay data presented in this study originate from two separate experiments carried out at the CERN isotope separator on-line device (ISOLDE) facility [7]. The thallium isotopes were predominantly formed through spallation reactions via protons, with an energy of 1.4 GeV and an intensity up to 2.1 μA, bombarding a 50 g cm^{-2} UC_x target. The proton beam consisted of a repeated sequence of pulses (typically 35–40) separated by (sometimes multiple) periods of 1.2 s, referred to as a supercycle. The thallium isotopes were resonantly laser-ionized in the hot-cavity using the same ionization scheme as used in the study of [26, 35]. The excitation from the atomic ground state to an intermediate electronic state 6d $^2D_{3/2}$ (36117.9 cm^{-1}) was performed by a frequency-doubled narrow-band tunable dye laser beam at 276.79 nm with a linewidth of 0.8 GHz. The subsequent ionization of excited thallium atoms was accomplished by a powerful 532 nm beam from a 10 kHz repetition rate edgewave frequency-doubled Nd:YAG laser, that was also used as a pump source for the first excitation step laser (for details of the RILIS laser setup see [29]). Thermal ionization of thallium in the hot cavity was also present, however it was approximately 20 times less efficient compared to laser ionization. After extraction from the ion source, acceleration to 30 keV and mass separation by the ISOLDE high resolution separator (^{182}Tl) or general purpose separator (^{184}Tl), a beam of the desired thallium isotopes was transported to the Windmill system [34–36] through a collimator and was then implanted in one of ten carbon foils (6 mm diameter, 20 μg cm^{-2} thickness [38]) mounted on a rotating wheel.

Two silicon (Si) detectors were placed at the implantation position in close geometry, covering a total solid angle of 24% of 4π. An annular silicon detector (Si1: total area 450 mm^2 including a hole of 8 mm diameter, thickness 300 μm) was placed upstream. The beam passed through the hole of 8 mm diameter. This detector was installed for the ^{184}Tl experiment, but it was absent when ^{182}Tl decay data were collected. Another circular silicon detector (Si2: total area 300 mm^2 and thickness 500/300 μm for ^{184}Tl/^{182}Tl measurements) was placed downstream behind the implantation foil. After each supercycle, the irradiated foil was rotated to move away the radioactivity from the implantation position. Longer-lived radiation was detected at the decay position with two circular silicon detectors placed in a similar manner as the implantation detectors (Si3/Si4 total area 300 mm^2, thickness of 300 μm placed downstream/upstream). In this way measurements at the decay station could be performed while implantation and measurements continued on a fresh foil in front of the ion beam. The energy resolution (full width half maximum, FWHM) of these detectors for α decays in the range of 5000–7000 keV was ~25–30 keV during the ^{184}Tl experimental campaign and ~35 keV during the ^{182}Tl campaign. The higher FWHM during the ^{182}Tl campaign is due to the fact that this run was dedicated to β-delayed fission (βDF) measurements, which require an energy range of the silicon detectors up to 100 MeV. The absolute efficiency for the Si detectors was determined with two ^{241}Am sources mounted on the wheel of the windmill and making use of α–γ coincidences between the 5485 keV ^{241}Am α decay and the 60 keV γ ray.

To detect γ rays, two single crystal high-purity germanium (HPGe) detectors were placed outside the vacuum chamber, downstream at 0° (Ge1, 90% purity, ~1 cm from the foil) and at 90° (Ge2, 70% purity, ~3 cm from the foil) with respect to the direction of the incoming beam. The typical energy resolution (FWHM) of each crystal for 1.3 MeV γ radiation was ~3.1 keV. Energy and efficiency calibrations were performed using standard calibrated sources of ^{133}Ba, ^{137}Cs, ^{60}Co, ^{241}Am and ^{152}Eu. The absolute photo-peak efficiency for the 506 keV line, the strongest transition in the internal transition (IT) decay of the (10$^-$) state in ^{184}Tl, was 4.9(1)% and 0.76(3)% in Ge1 and Ge2 respectively, for the given geometry. Due to the combination of a high γ-multiplicity in the β decay of ^{182}Tl and ^{184}Tl and close-detector

configuration, the effective efficiency for the HPGe detectors was lower than that determined by the efficiency calibration using standard calibrated sources. To account for this effect, the efficiency for the 351 and 367 keV γ lines, the $2^+ \rightarrow 0^+$ transition in the β-decay daughters ^{182}Hg and ^{184}Hg respectively, has been determined by γ-γ coincidences. With this method, an efficiency for the 351 keV line in ^{182}Hg of 0.77(7)% and 0.44(4)% was obtained for Ge1 and Ge2 respectively. For the 367 keV line in ^{184}Hg, efficiencies of 2.0(2)% and 0.71(7)% were obtained for Ge1 and Ge2 respectively. The difference in effective efficiency is due to the higher multiplicity in the β decay of ^{182}Tl compared to ^{184}Tl.

In the detection setup, digital electronics (digital gamma finder) modules [39]) were used to acquire the data [35]. The data were collected event by event and independently time stamped. The event coincidences and time structure were reconstructed by software analysis.

3. Results

3.1. ^{184}Tl

During the experimental campaign, three different data sets were collected on mass 184. In the first data set, the thallium atoms were ionized only through surface ionization. This data set is denoted further as surface ionized (SI) data. A second data set consists of laser scans, where decay spectra were taken as a function of the first excitation step laser frequency. A third data set was acquired where the first excitation step laser frequency is tuned in order to selectively enhance the production of the (10^-) state and, through its IT, also the (7^+) state relative to the (2^-) state. This data set is denoted further as laser ionized (LI) data. In the SI α- and β-decay data set, the ^{184}Tl beam is composed of 61(1)% (2^-) and 39(1)% (7^+) states, while in the LI α-and β-decay data set this is 20(1)% (2^-) and 80(1)% (7^+) states respectively. For a more detailed description of this LI data set we refer the reader to [12]. Combining the different data sets enables to disentangle the decay schemes of the three long-lived states in ^{184}Tl [12, 37], namely, the α decay and IT of the (10^-), the α and EC/β^+ decay of the (7^+) and the (2^-).

Figure 1 shows the singles α-decay energy spectra for mass 184 collected at the implantation position. Spectra 1(a) and (b) correspond to the LI and SI data sets respectively. The strongest peaks in both spectra are due to known α decays of the isotopes ^{184}Tl and ^{184}Hg, the latter being populated in the β decay of ^{184}Tl. The 5539(5) keV α line from ^{184}Hg and 5987(4) and 6161(4) keV α lines from ^{184}Tl are used for energy calibration [25]. It should be noted however that the α-decay peaks originating from ^{184}Tl are broadened compared to the peak from ^{184}Hg due to α-electron (α-e$^-$) summing effects, where the energy of the α decay, feeding an excited state, which decays by an (at least, partially) converted γ transition, may sum up with the energy of the subsequent conversion electron if both are registered by the same detector. Such summing effects have also been discussed in [43–45] and we refer to these papers for more details. This summing effect makes the determination of the α-decay energy for the affected peaks difficult and large systematic uncertainties are necessarily introduced on these energy values. Some weaker peaks originating from the α decay of ^{180,184}Au are also identified. The nucleus ^{184}Au is populated in the β decay of ^{184}Hg, while ^{180}Au is, as will be shown later, mainly populated through the α decay of the (2^-) state of ^{184}Tl. A marked difference between both spectra is visible in the extra tail around 6200 keV and the increased intensity around 5650 keV in the LI data, spectrum 1(a). In the following sections we will focus on the α decay of the three long-lived states in ^{184}Tl.

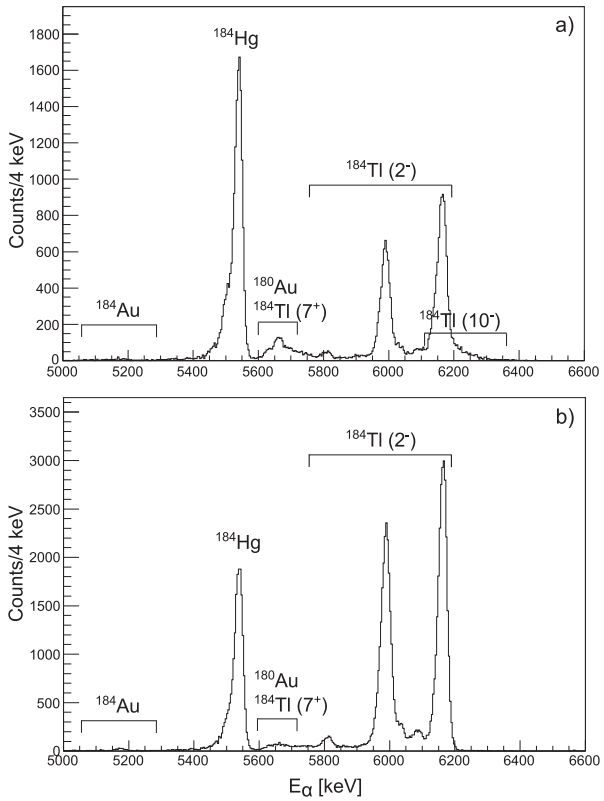

Figure 1. Relevant part of the singles α-decay energy spectrum collected at the implantation position (sum of Si1 and Si2). Spectra (a) and (b) correspond to the LI and SI data sets respectively. The α peaks are denoted with the isotope (and possible spin) to which they belong. The peaks at 5539(5), 5109(5), 5187(5), 5648(10) keV originate from the known α decays of ^{184}Hg, ^{184}Au, ^{184}Au, ^{180}Au respectively [40–42].

3.1.1. α decay of the (10^-) isomeric state. In the LI data set, the production of the (10^-) and (7^+) states is selectively enhanced relative to the production of the (2^-) state. From the time distribution of the events in the IT of the (10^-) state a half-life of 47.1(7) ms was extracted in our complementary study [12], while the half-lives of the (7^+) and (2^-) states are in the order of $\sim$10 s [8, 9, 14]. Using this difference in half-life between the (10^-) and $(7^+, 2^-)$ states within the LI data set, an α-decay energy spectrum containing only α decays associated with the decay of the (10^-) isomeric state can be produced. The pulsed structure of the proton beam together with the short implantation time after each proton pulse enables this discrimination. Figure 2 shows a purified (10^-) singles α-decay energy spectrum obtained by subtracting from the singles α-decay energy spectrum collected between 10 and 200 ms after each proton pulse, the singles α-decay energy spectrum collected after 200 ms. Normalization is performed by matching the intensity of the 367 keV γ line in the singles γ-ray energy spectra obtained under the same conditions (see [12]). The 367 keV γ line is the $2^+ \rightarrow 0^+$ transition in ^{184}Hg observed in the β decay of the (7^+) and (2^-) states. In the singles α-decay energy spectrum of figure 2 an α line at 6132 keV originating from the (10^-) isomeric state is

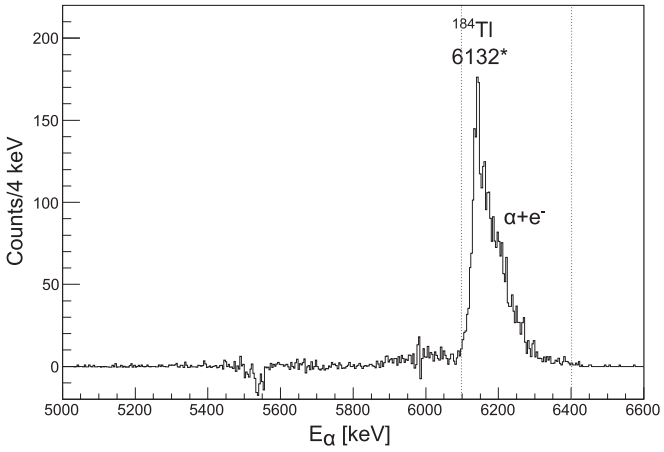

Figure 2. Relevant part of the purified α-decay energy spectrum from the (10^-) isomeric state in ^{184}Tl collected in Si1 and Si2. The α-decay energy is denoted in keV. The vertical dashed lines indicate the gate used for α–γ coincidences (see figure 3) (*: energy determined from α–γ coincidences).

identified. The high-energy tail originates from α-e$^-$ summing. From the time distribution of the events in the α peak, a half-life of 46.5(52) ms is extracted which is consistent with the half-life of 47.1(7) deduced from the IT of the (10^-) state [12]. The purity of the spectrum of figure 2 allows the determination of the α-decay branching ratio for this isomeric state. By comparing the intensity of the 6132 keV α decay and the 506 keV γ ray of the (10^-) state, an α-decay branching ratio of 0.089(19)% is deduced, using an absolute γ-decay branching ratio of 70(3)% of the 506 keV γ transition [12]. Using the Rasmussen formalism [46] this leads to a reduced α-decay width of 16(4) keV, indicating an unhindered α decay to a state in daughter ^{180}Au.

Figures 3(a) and (b) show the α–γ coincidence matrix and the projection on the γ-energy axis focussing on the (10^-) isomeric state, using a prompt coincidence window of 500 ns. Both spectra are produced using the LI data set and selecting events collected between 10 and 200 ms after each proton pulse. For the (10^-) state, one can distinguish five groups of α–γ coincident events. The α line at 6132 keV is seen in coincidence with four main γ lines at 101, 108, 163 and 206 keV and Au K x-rays. Comparison of the peak intensity ratio in the Au K x-ray region with the theoretical K_α/K_β ratio reveals a γ transition of about 78 keV buried under the Au K_β x-rays. At the right-hand side of the α peak in the singles spectrum of figure 2 a tail is present. This tail originates from the previously mentioned α-e$^-$ summing effects. The 78, 101, 108 and 163 keV γ rays are seen in prompt coincidence with these α-e$^-$ summed events, which indicates that these transitions decay most probably as part of different cascades. However, the 206 keV γ line is only coincident with the low-energy part of the α peak and not with the α-e$^-$ tail. This observation suggests that the 206 keV γ line probably feeds a long-lived state in daughter ^{180}Au. No de-exciting γ rays of this state were seen in coincidence with the (10^-) α line using a (delayed) coincidence gate up to 1 ms. The prompt coincidence condition limits the possible multipolarity of all five γ rays to E1, M1 or E2. An overview of the observed α decays and coincident γ rays for the (10^-) isomeric state is given further in table 1. Due to the limited statistics and lack of knowledge about the structure of daughter isotope ^{180}Au, only a partial α-decay scheme can be constructed for this isomeric state (see discussion).

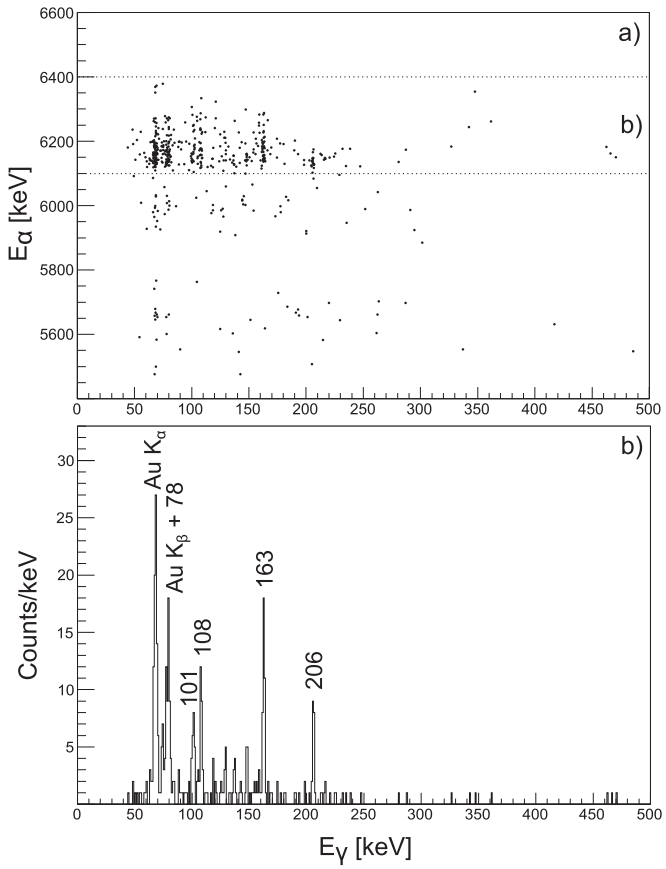

Figure 3. (a) The prompt α–γ coincidence matrix at mass 184, collected between 10 and 200 ms after each proton pulse, using the LI data set. (b) The projection on the γ-energy axis for the events between the horizontal dashed lines corresponding to the (10^-) state (see also figure 2). The energy of the coincident γ rays is indicated in keV.

3.1.2. α decay of the (7^+) isomeric state. To discriminate between the decay of the (7^+) and (2^-) states, one can combine the SI and LI data sets. Within both data sets only events are selected that are collected from 200 ms after the proton pulse until the next proton pulse to eliminate the activity from the short-living (10^-) state. As mentioned in the previous section, in the LI data set the activity from the (7^+) is enhanced over that of the (2^-) state compared to the SI data. The purified (7^+) α-decay energy spectrum in figure 4 results from the subtraction of the singles α-decay energy spectrum in the SI data from the singles α-decay energy spectrum in the LI data, after normalization using the 6161 keV α-decay intensity that originates from the α decay of the (2^-) state in ^{184}Tl. Using the same procedure, a purified (7^+) γ-ray spectrum can be obtained (see also [37]). In figure 4 an α line at 5659 keV, together with an α-e$^-$ tail, originating from the (7^+) isomeric state in ^{184}Tl is identified. The peak at 5539 keV originates from the α decay of ^{184}Hg, now exclusively fed through the β decay of the (7^+) state in ^{184}Tl. The half-life of the (7^+) isomeric state can not be determined due to the presence of an α line from the α-decaying daughter ^{180}Au that has a similar α-decay energy of 5648 keV and 8.1(3) s half-life [42] in the singles α-decay energy spectrum (see figure 1). To calculate the reduced α-decay width the literature value of 11(1) s [9] is

Table 1. Overview of ^{184}Tl α decay, including the different isomers and corresponding α-decay branching ratio b_α, energy E_α, intensity I_α from purified singles spectra (Si1–2), relative intensity I_α from purified singles spectra (Si1–2), reduced α-decay width δ_α^2 and γ rays observed in coincidence (Si1–2 with Ge1). The sum $Q_\alpha + E_\gamma$ is also given for a number of transitions. The uncertainties are indicated between brackets and include both statistical and systematic contributions.

J^π, b_α (%)	E_α (keV)	I_α (counts)	$I_{\mathrm{rel},\alpha}$ (%)	δ_α^2 (keV)	E_γ (keV)	$Q_\alpha + E_\gamma$ (keV)
(10^-), 0.089(19)	6132(19)[a]	3181(60)	100	16(4)	205.9(2)	6474(19)
					162.6(1)	
					107.9(2)	
					101.3(6)	
					∼78[e]	
					Au K_β	
					Au K_α	
(7^+), 0.047(6)	5659(10)[a]	1678(49)	100	4.9(12)	363.3(6)	6148(10)
					261.8(3)	
					257.7(3)	
					175.7(3)	
					∼78[e]	
					Au K_β	
					Au K_α	
(2^-), 1.22(30)	6161[b]	19020 (206)	93(1)	0.57(6)		6298
	5988(12) +5964(12)[c]	20390 (217)[d]	100	2.4(4)		
	5964(13)[a]				224.3(3)	6321(13)
	5988(12)[a]				201.3(3)	6322(12)
					184.2(1)	6305(12)
					178.5(1)	
					126.3(1)	
					Au K_β	
					Au K_α	
	5810(12)[a]	1232(57)	6.0(3)	0.9(1)	365.1(2)	6304(12)
					315.1(2)	
					272.8(3)	
					198.4(9)	
					Au K_β	
					Au K_α	
	5748(12)[a]	<73	<0.4	<0.09	426.0(5)	6302(12)

[a] E_α from α–γ coincidences.
[b] E_α used to calibrate the silicon detectors.
[c] Dominant contribution from 5988(12) α line.
[d] I_α for range indicated by vertical dashed lines in figure 6.
[e] Determined by substracting the Au K_β intensity, calculated from the Au K_α-line intensity.

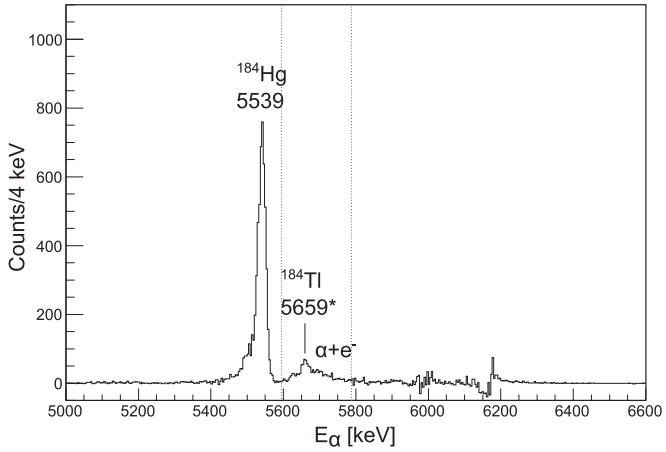

Figure 4. Relevant part of the purified α-decay energy spectrum from the (7^+) isomeric state in ^{184}Tl, collected in Si1 and Si2. The α-decay energies are denoted in keV. The vertical dashed lines indicate the gate used for α–γ coincidences (see figure 5). (*: energy determined from α–γ coincidences).

used for the half-life. An α-decay branching ratio of the (7^+) state of 0.047(6)% is deduced by comparing the α-decay intensity in the purified (7^+) α-decay energy spectrum with the intensity of the 367 keV $2^+ \rightarrow 0^+$ transition in ^{184}Hg in the purified (7^+) γ-ray energy spectrum. An absolute β-decay branching ratio of 90(2)% of this transition in the (7^+) β decay, as reported in [37], is used. Using the Rasmussen formalism [46], a reduced α-decay width of 4.9(12) keV is determined, indicating a hindered character of the 5659 keV α decay to a level in ^{180}Au.

In figure 5 the α–γ coincidence matrix focussed on the (7^+) isomeric state is shown in 5(a) and the corresponding projection on the γ-energy axis in 5(b). A prompt coincidence window of 500 ns is used. Both spectra are produced using the LI data set and selecting events collected from 200 ms after the proton pulse on until the next proton pulse. It should be noted that some events originating from the (2^-) α decay are also observed, due to surface ionization which is always present (see earlier). Five groups of α–γ coincident events can be identified. The γ lines at 363, 262, 258, 176 and Au K x-rays are seen in coincidence with the α line at 5659 keV. Also in this case a γ transition of 78 keV buried under the Au K_β x-rays is revealed when comparing the peak intensity ratio in the Au K x-ray region with the theoretical K_α / K_β ratio. Due to the limited statistics and lack of knowledge about the structure of daughter isotope ^{180}Au, only a partial α-decay scheme can be constructed for this isomeric state (see discussion). An overview of the observed α decays and coincident γ rays for the (7^+) state is given in table 1.

3.1.3. α decay of the (2^-) isomeric state. Using a similar procedure as in the case of the (7^+) isomeric state, a singles α-decay energy spectrum containing only α decays associated with the decay of the (2^-) state can be produced. The spectrum in figure 6 results from the subtraction of the singles α-decay energy spectrum in the LI data from the singles α-decay energy spectrum in the SI data, after normalization on the 340 keV γ line. The latter is the $6^+ \rightarrow 4^+$ transition in ^{184}Hg and is predominantly fed by the (7^+) β decay in ^{184}Tl. Also for the (2^-) state, singles γ-ray energy spectra are produced using the same purification procedure. It should be noted that a normalization factor using the α intensity of the (7^+) peak

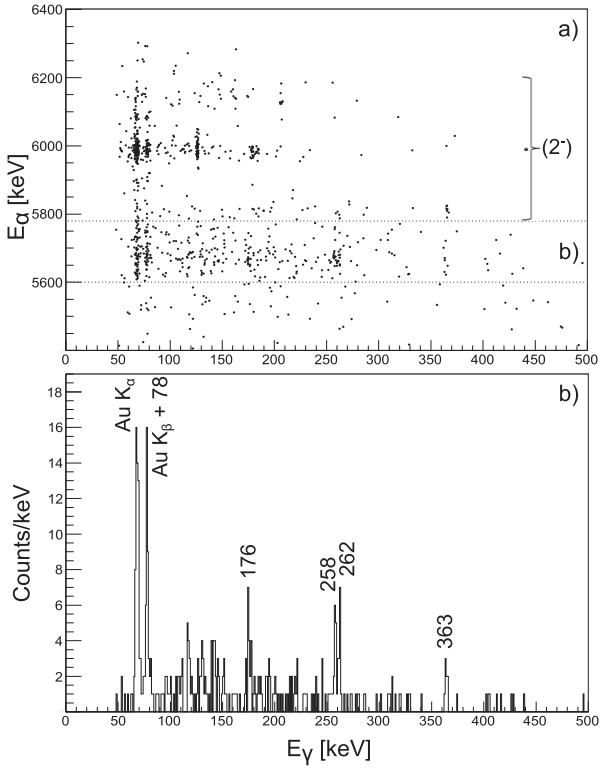

Figure 5. (a) The prompt α–γ coincidence matrix at mass 184, using the LI data and selecting events collected from 200 ms after the proton pulse. (b) The projection on the γ-energy axis for the events between the horizontal dashed lines defining the (7^+) events (see also figure 4). The energy of the coincident γ rays is indicated in keV.

cannot be used due to the presence of the ^{180}Au α line and possibly α intensity from the (2^-) decay buried under that of the ^{184}Tl (7^+) (see figure 1). The peak at 5539 keV originates from the α decay of ^{184}Hg, fed by the β decay of the (2^-) state in ^{184}Tl. The previously suggested [8] α lines decaying from the (2^-) state in ^{184}Tl, seen in our work at 5810, 5988, 6161 keV are indicated in the singles spectrum from figure 6.

Figures 7(a) and (b) show the time distribution of the events in the 5950–6010 and 6140–6200 keV α lines from the (2^-) isomeric state respectively. Data are collected at the decay position (Si3 and Si4) and are not affected by the incoming beam. The dotted red line results from a fit of a simple exponential function to the data resulting in half-life values of 9.4 (2) s and 9.6(2) s for (a) and (b) respectively, which leads to a mean value of 9.5(2) s.

The α-decay branching ratio of the (2^-) state is deduced by comparing the intensity ratio of the total number of α decays attributed to ^{184}Tl (7^+) or (2^-) relative to the number of α decays from ^{184}Hg in respectively the purified (7^+) and (2^-) spectra. By using the measured α-decay branching ratio of the (7^+) state (0.047(6)%), an α-to-β normalization factor can be deduced between the number of α particles from the (7^+) decay and from ^{184}Hg (β daughter of ^{184}Tl). As the (2^-) and (7^+) half-lives are similar, the same normalization can be used to deduce the α-branching ratio of the (2^-) decay, resulting in a value of 1.22(30)%. This value includes a systematic uncertainty of 20% to take into account a possible difference in half-life

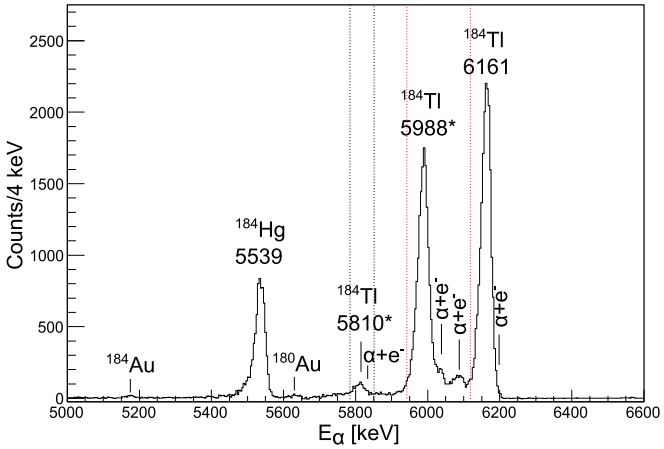

Figure 6. Relevant part of the purified α-decay energy spectrum from the (2^-) isomeric state in ^{184}Tl, collected in Si1 and Si2. The α-decay energies are denoted in keV. The vertical dashed lines indicate the gates used in α–γ coincidence analysis (see figure 8) (*: energy determined from α–γ coincidences).

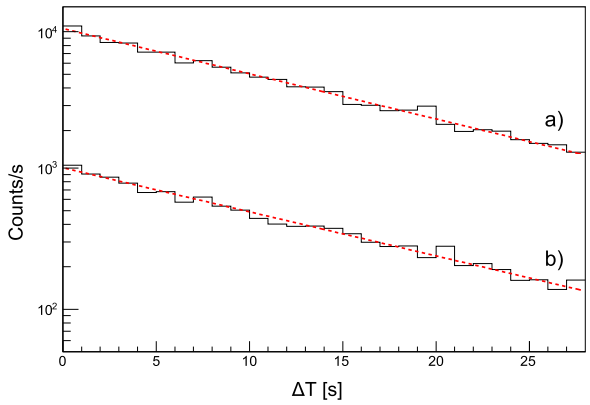

Figure 7. (a) and (b) show the time distribution of the events in the 5950–6010 and 6140–6200 keV α lines from the (2^-) isomeric state respectively, collected at the decay position (Si3 and Si4). The data indicated with (a) are upscaled by a factor of ten for visualization purposes. The dotted red lines result from a fit of a simple exponential function to the data.

between the (2^-) and (7^+) states. Using the Rasmussen formalism [46] reduced α-decay widths are calculated for the different decay branches. These results will be discussed further.

More α lines are identified by detailed α–γ coincidence analysis (see table 1). Figure 8 shows the prompt α–γ coincidence matrix focussed on the (2^-) isomeric state and two projections on the γ-energy axis corresponding to the two regions between the horizontal dashed lines in the α–γ coincidence matrix. All spectra are produced using the SI data set, an α–γ prompt window of 500 ns and selecting events collected from 200 ms after the proton pulse on until the next proton pulse. No coincidence relation between the α line at 6161 keV and any γ rays is observed. An overview of the observed α decays and coincident γ rays for the (2^-) state is given in table 1. Owing to the complexity of the α-decay pattern and limited

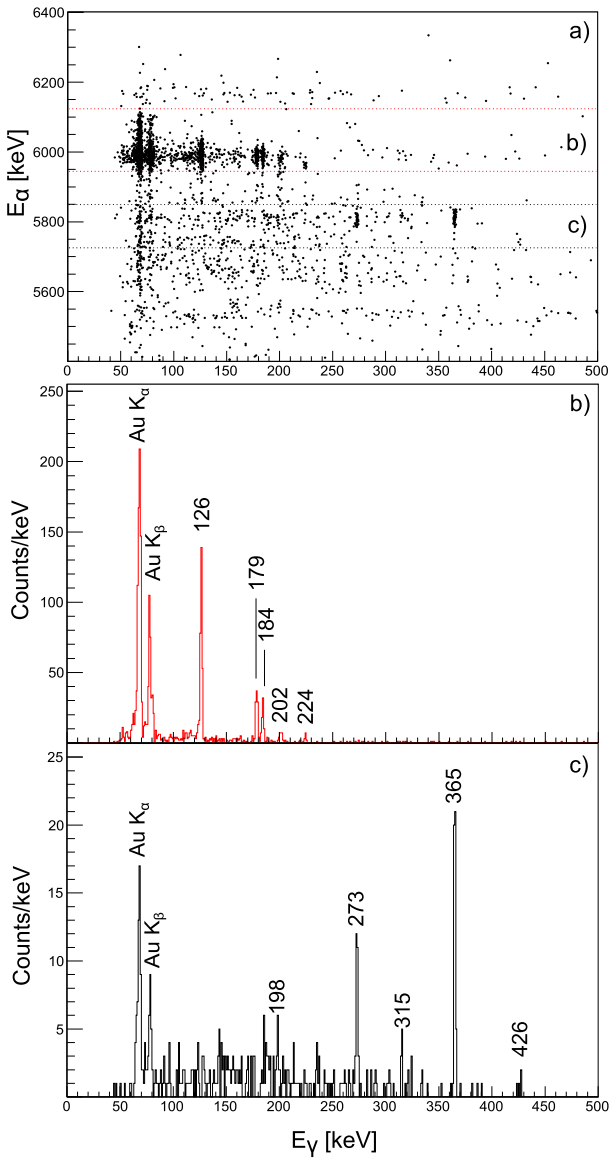

Figure 8. (a) The prompt α–γ coincidence matrix at mass 184, using the SI data and selecting events collected from 200 ms after the proton pulse. (b) and (c) projections on the γ-energy axis for the events between the horizontal dashed lines defining the (2^-) events (see also figure 6). The energy of the coincident γ rays is indicated in keV.

knowledge on the structure of daughter isotope ^{180}Au, only a partial α-decay scheme can be constructed (see discussion).

3.2. ^{182}Tl

Figure 9 shows the relevant part of the singles α-decay energy spectrum taken at mass 182. Five α lines are assigned to the decay of ^{182}Tl (see further) and are indicated in figure 9. Only

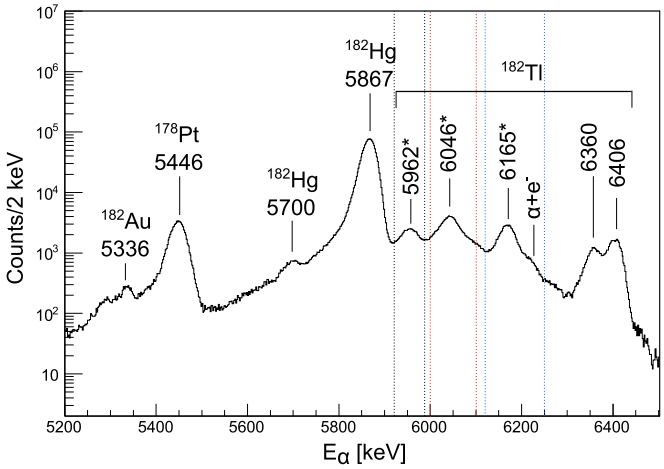

Figure 9. Relevant part of the α-decay energy spectrum at the implantation position measured at mass 182 (Si2). The α-decay energies are denoted in keV. The vertical dashed lines indicate the gates used in α–γ coincidence analysis (see figure 11). The peaks at 5700(8), 5867(5), 5336(8) and 5446(6) keV originate from the known α decay of ^{182}Hg, ^{182}Hg, ^{182}Au and ^{178}Pt, respectively [41, 42, 47–49]. (*: energy determined from α–γ coincidences).

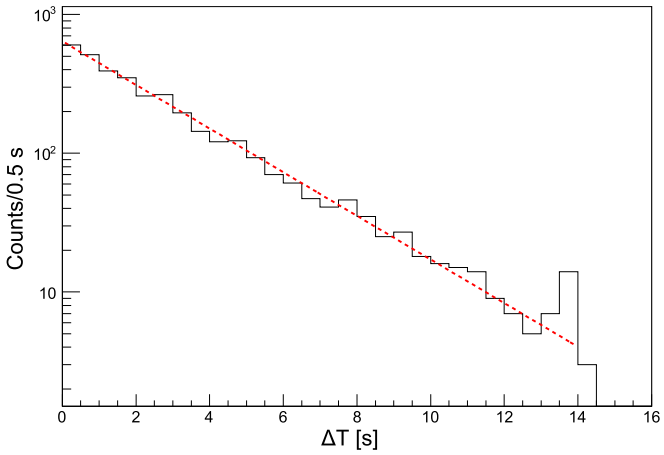

Figure 10. Time distribution of the events in the 6360 and 6406 keV ^{182}Tl α lines, collected at the decay position (Si3 and Si4). The dotted red line shows the result of a fit by an exponential curve resulting in the half-life value of 1.9(1) s.

the ^{182}Tl peaks observed in our work at 6046 and 6406 keV are known from literature [13, 14]. The other peaks in figure 9 originate from the α decay of ^{182}Hg, ^{178}Pt and ^{182}Au, all expected decay products of ^{182}Tl. The 5446(3), 5867(5) and 6406(10) keV α lines from ^{178}Pt, ^{182}Hg and ^{182}Tl, respectively, are used for calibration [25]. From the time distribution of the events in the peaks at 6360 and 6406 keV, a half-life of 1.9(1) s has been extracted (see figure 10). This is noticeably smaller and more precise than the previously reported values of 2.8(6) s [14] and 3.1(10) s [15] from α-and β-decay data respectively, but agrees with the value of 2.0(3) s reported by [14] deduced from a β-decay study. The half-lives determined

from the other three peaks are consistent with the value of 1.9(1) s, supporting their assignment to ^{182}Tl.

In accordance with the results of the α-decay study of ^{186}Bi [6], clear evidence was found for the presence of two isomeric states in ^{182}Tl from β-decay studies [37]. The hyperfine structure patterns for different α- and γ-lines in the ^{182}Tl decay spectra, obtained in narrow-band laser scans, strongly support this observation [27]. The hyperfine structure pattern of the $8^+ \rightarrow 6^+$ (413 keV) and $6^+ \rightarrow 4^+$ (332 keV) γ transitions in β-decay daughter ^{182}Hg, as a function of laser frequency is distinctly different from the pattern of the $2^+ \rightarrow 0^+$ (351 keV) transition, indicating a high-spin β-decaying state and a low-spin β-decaying state. All α lines in our study have a hyperfine structure pattern testifying to the predominance of the low-spin state decay in these lines. Out of the narrow-band laser scans, there is evidence for α decay from the high-spin state in the region around 6250 keV, however no further information can be extracted. We refer the reader to [27] for a more detailed description of the hyperfine structure of these two decaying states in ^{182}Tl. In the complementary β-decay study of the same data set [37], it was not possible to disentangle the two β-decay schemes. As a consequence, we are only able to deduce a lower limit for the α-branching ratio of the low-spin state in ^{182}Tl. This lower limit of 0.49% is deduced by comparing the ^{182}Tl intensity in the singles α spectrum with the intensity of the 351 keV $2^+ \rightarrow 0^+$ transition in ^{182}Hg in the singles γ spectrum, using the absolute β-branching ratio of 74(3)% of this transition in the β decay from [37]. This lower limit for the branching ratio is the edge within which 95% of the events will be found.

During the experimental campaign, one of the goals was to search for the βDF decay of ^{182}Tl. However, no fission events are observed in this data set. Considering that less than one βDF fission event is observed, a lower limit for the βDF partial half-life [50] $T_{l/2p,\beta DF} > 5.2 \times 10^7$ s is extracted and the upper limit for the βDF probability [50] is given by $P_{\beta DF} < 3.4 \times 10^{-8}$. These values are also the edge within which 95% of the events will be found. From the systematic behavior of $T_{l/2p,\beta DF}$ with respect to the difference between the parent Q-value for β decay Q_β and the daughter fission barrier B_f, Q_β–B_f, presented in [51], a $T_{l/2p,\beta DF}$ value in the order of 10^5–10^6 s is expected for ^{182}Tl. The experimental lower limit for $T_{l/2p,\beta DF}$ in the βDF decay of ^{182}Tl is thus more than two orders of magnitude larger than the estimated values from systematics [51]. However, it should be noted that $T_{l/2p,\beta DF}$ and $P_{\beta DF}$ are calculated, similar to the α-branching ratio, using the 351 keV $2^+ \rightarrow 0^+$ transition in ^{182}Hg which contains both low-and high-spin contributions. Consequently, the lower and upper limit for $T_{l/2p,\beta DF}$ and $P_{\beta DF}$ respectively, are only overall values since it is not possible to differentiate between the two isomers. Further experimental work to investigate these findings by producing isomerically purified radioactive ion beams is underway.

Figure 11(a) shows a prompt α–γ coincidence matrix for ^{182}Tl while the corresponding projections on the γ-energy axis are given in spectra 11(b)–(d). We can identify different groups of α–γ coincident events using a prompt timing window of 500 ns. An overview of the observed α decays and coincident γ rays for ^{182}Tl is given in table 2. No coincidence relation between the two α lines at 6406 and 6360 keV and any γ rays is observed (see figure 11(a)). However, the difference in Q_α between these α decays is 46 keV which is below the detection limit of our HPGe detectors. Due to the complexity of the α-decay pattern of this odd–odd nucleus and limited knowledge about the structure of daughter isotope ^{178}Au, only a limited α-decay scheme can be constructed (see discussion).

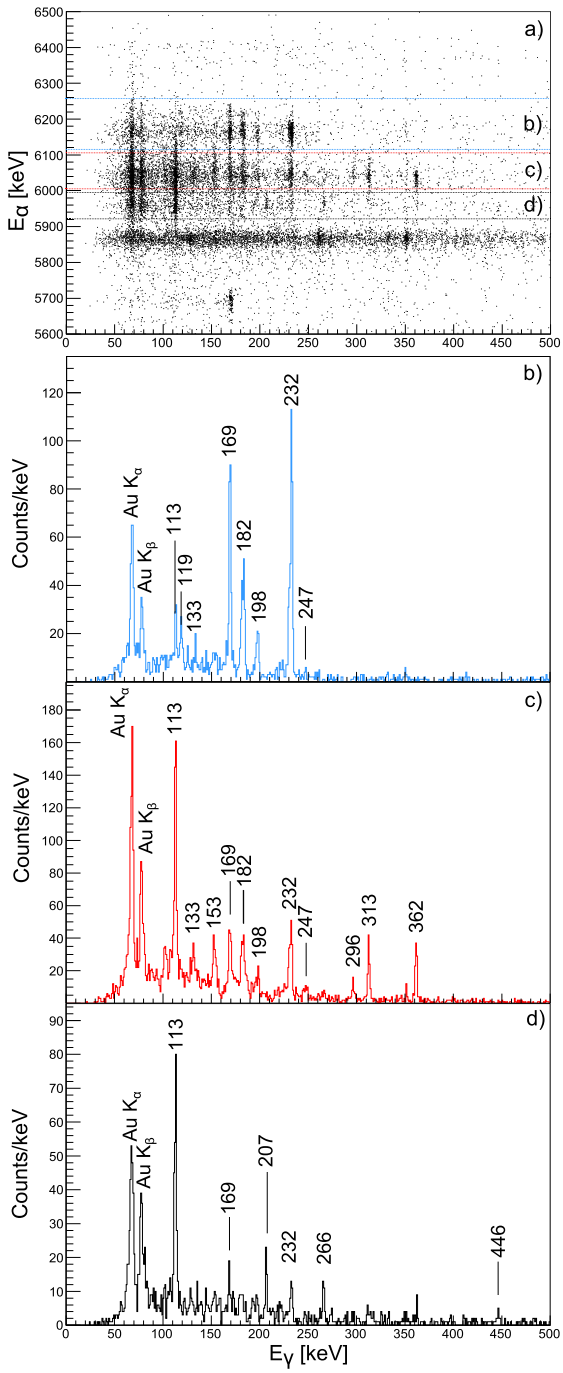

Figure 11. (a) the prompt α–γ coincidence matrix for mass 182. (b), (c) and (d) projections on the γ-energy axis for the events between the horizontal dashed lines corresponding to the different α–γ groups in spectrum (a) (see also figure 9). The energy of the coincident γ rays is indicated in keV. The events in spectrum (a) around 5700 keV are from fine structure in the α decay of ^{182}Hg.

Table 2. Overview of ^{182}Tl low-spin α decay, including the α-decay branching ratio b_α, energy E_α, intensity I_α (Si2), relative intensity I_α (Si2), reduced α-decay width δ_α^2 and γ rays observed in coincidence (Si2 with Ge1). The sum $Q_\alpha + E_\gamma$ is also given for a number of transitions. The uncertainties are indicated between brackets and include both statistical and systematic contributions.

b_α (%)	E_α (keV)	I_α (counts)	$I_{rel,\alpha}$ (%)	δ_α^2 (keV)	E_γ (keV)	$Q_\alpha + E_\gamma$ (keV)
>0.49	6406[a]	9367(97)	21(3)	>0.017		6550
	6360(6)	7301(85)	16(3)	>0.019		6503(6)
	6165(6)[b]	28080(168)	62(10)	>0.45	247.2(5)	6551(6)
					232.2(1)	
					197.5(2)	6501(6)
					182.3(2)	
					169.2(1)	
					132.9(4)	
					118.7(3)	
					112.9(2)	
					Au K_β	
					Au K_α	
	6046(5)[b]	45500(213)	100	>2.3	361.5(1)	6543(6)
					312.6(1)	
					296.7(3)	
					247.8(7)	
					231.8(2)	
					197.5(8)	
					182.7(3)	
					169.3(2)	
					153.4(2)	
					131.7(4)	
					112.9(1)	
					102.0(5)	
					Au K_β	
					Au K_α	
	5962(5)[b]	20520(143)	45(7)	>2.4	446.1(14)	6542(5)
					265.8(2)	
					232.2(3)	
					206.7(1)	
					169.2(3)	
					112.9(1)	
					Au K_β	
					Au K_α	

[a] E_α used to calibrate the silicon detectors.
[b] E_α from α–γ coincidences.

4. Discussion

The partial α-decay schemes depicted in figure 12 for the ^{184}Tl (10^-) and (7^+) states are constructed using the information from table 1 and the excitation energy (506 keV) of the (10^-) intruder state relative to the (7^+) state [12]. The 6132 keV (10^-) α decay has a reduced

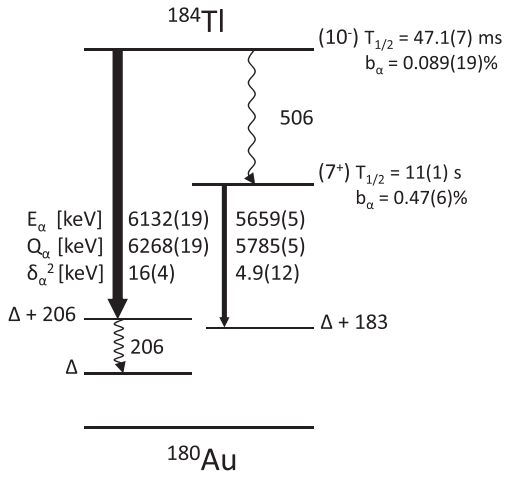

Figure 12. Partial α-decay scheme for the (10^-) and (7^+) states in ^{184}Tl. The E_α, Q_α values and corresponding reduced α-decay widths δ^2_α are indicated next to the corresponding α decays, together with the energy of selected observed coincident γ rays.

α-decay width of 16(4) keV. The unhindered α decays in the odd-mass neighbors ^{183,185}Tl involving the $\pi 1h_{9/2}$ intruder orbitals have reduced α-decay widths of about 30 keV [8, 10, 52, 53]. The presumed intruder-based $[\pi 1h_{9/2} \otimes \nu 1i_{13/2}\ ]$ (10^-) state is thus α decaying moderately hindered by a factor of $\sim$2, relative to the unhindered α decays of neighboring ^{183,185}Tl isotopes. This hints to the influence of an extra unpaired neutron in the odd–odd ^{184}Tl case and indicates that the (10^-) α-decaying state in ^{184}Tl and the excited state at the level $\Delta + 206$ keV in figure 12, fed in ^{180}Au have a similar structure. Intruder states of $\pi 1\, h_{9/2}$ origin have been identified in heavier odd–odd ^{182,184,186}Au, which supports also its possible presence in ^{180}Au. The state at $\Delta + 206$ keV in ^{180}Au, fed in the α decay of the (10^-) state, decays further by a number of γ rays of which the 206 keV is the highest in energy. As can be seen in figure 3(a), the feeding α line of 6132 keV does not have an α-e$^-$ tail, pointing to the existence of an isomeric level Δ fed by the 206 keV γline. Based on the α–γ data of the (7^+) state, the level Δ cannot be the groundstate (see below). As mentioned above, the other four γ rays are seen in prompt coincidence with the summed α-e$^-$ tail and are thus most probably decaying as part of different cascades from the level $\Delta + 206$ keV. A possible crossover α-decay branch from the (10^-) to the state labeled Δ in figure 12 is not observed, which leads to an upper limit of its reduced α-decay width of 0.014 keV. The presumed regular $[\pi 3s_{1/2} \otimes \nu 1i_{13/2}\ ]$ (7^+) decays with a reduced α-decay width of 4.9(12) keV to an excited state in ^{180}Au, labeled $\Delta + 183$ in figure 12, which further decays by a number of γ transitions from which the 363 keV is the highest in energy. This points to the existence of a number of levels below the level labeled Δ. However, no further conclusions can be drawn with respect to decays to the ^{180}Au ground state.

In figure 13 the partial α-decay scheme for the ^{184}Tl (2^-) state is given. The reduced α-decay widths range from 0.09 to 2.3 keV, indicating that all α-decay branches of this isomeric state are hindered. The 6161 keV transition is the α line with the highest energy in the decay of the (2^-) state. However, α–γ coincidences establish a level, labeled x, 17.1(3) keV lower than the level fed by the 6161 keV line and this α decay is thus not the crossover transition. The 6161 keV α line is broader at the right-hand side relative to the ^{184}Hg α-decay peak,

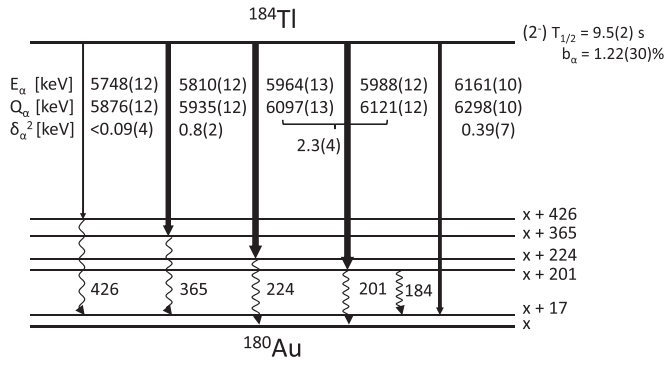

Figure 13. Partial α-decay scheme for the (2^-) state in ^{184}Tl. The E_α, Q_α values and corresponding reduced α-decay widths δ^2_α are indicated next to the corresponding α decays, together with the energy of selected observed coincident γ rays.

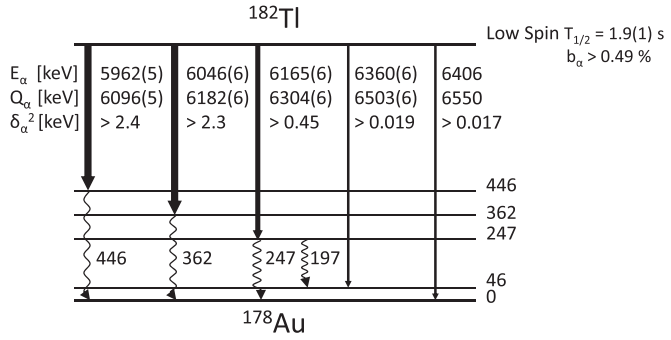

Figure 14. Partial α-decay scheme for the low-spin state in ^{182}Tl. The E_α, Q_α values and corresponding reduced α-decay widths δ^2_α are indicated next to the corresponding α decays, together with the energy of observed coincident γ rays.

which indicates also here α-e$^-$ summing. This can be considered as additional evidence for the level at 17.1(3) keV, since the conversion electrons depopulating this level may sum up with the 6161 keV α line if both are registered simultaneously in the same silicon detector. It cannot be concluded that the level x is the ground state of ^{180}Au. Combining the information of the three α-decaying states in ^{184}Tl, there is evidence of at least two long-living states (the states x and Δ) in ^{180}Au.

In the partial α-decay scheme of ^{182}Tl in figure 14 one can distinguish three groups of decays, based on their similar reduced α-decay widths. It should be noted that, since the α-decay branching ratio of 0.49% is a lower limit, the reduced α-decay widths are lower limits as well. The α-decay transitions with energies of 5962 and 6046 keV both have reduced α-decay widths of about 2.5 keV. This points to a similar structure of the two excited levels at 446 and 362 keV in daughter ^{178}Au. The α decay of 6165 keV feeding a level at 247 keV has a reduced α-decay widths of 0.45 keV, a factor of $\sim$5 more hindered compared to the 5962 and 6046 keV α decays. However, the 6360 keV and full-energy 6406 keV transitions are much more hindered ($\delta^2 \approx 0.02$ keV), a factor of 130 relative to the 5962 and 6046 keV α decays and 25 relative to the 6165 keV. The similar reduced widths of the strongly hindered

transitions to the (supposed) ground state and excited level at 46 keV indicate also to the similar structure of both levels.

The hyperfine structure pattern of the α-decaying state in ^{182}Tl is similar to that of ^{180}Tl [27], for which a spin assignment $I = 4, 5$ was proposed in [26]. Based on this argument and the close values of the corresponding magnetic moments, it is tempting to assign to these states the same spin and configuration [27]. As mentioned in the introduction, a neutron configuration change to $[\pi 3s_{1/2} \otimes \nu 1h_{9/2}]_{4^-,5^-}$ can be expected to occur around ^{180,182}Tl. Long-living states with this assumed structure have been identified in ^{178,180}Tl [54, 55]. In the α decay from this state in ^{180}Tl, five α lines have been observed by Toth *et al* [55] and recently also by Kondev *et al* [56]. The two lowest energy α transitions, 6208 and 6281 keV, have reduced α-decay widths of 4.9(36) and 4.2(29) keV respectively, which corresponds remarkably well to the situation in ^{182}Tl, confirming the probably identical structures of the parent states in both isotopes. Also in ^{178}Tl, the two α lines with the lowest energy values, decay unhindered to excited levels in ^{174}Au [54]. The broad range in reduced α-decay widths from almost no hindrance to a hindrance of about 2000 relative to oddthallium neighbors, which could be determined because of the high statistics obtained, points to strong structural changes between parent thallium and daughter gold isotopes. 182Tl is characterized by rather pure nearly spherical states involving proton-holes in the $Z = 82$ shell, while the respective gold isotope is strongly deformed [57].

5. Conclusion

The α decay of ^{182,184}Tl was studied at the ISOLDE facility. The α decay of the three long-lived states in ^{184}Tl, (10^-), (7^+) and (2^-), has been disentangled and for the first time, α-decay branches for the (10^-) and (7^+) states were identified. Due to the purity of the singles α-decay energy spectra for all three states, α-decay branching ratios of 0.089(19)%, 0.047 (6)% and 1.22(30)% were extracted for the (10^-), (7^+) and (2^-) states respectively. A more precise half-life of 9.5(2) s was deduced for the (2^-) state. New α-decay lines were identified also for ^{182}Tl, all of them have a half-life of 1.9(1) s. A lower limit of the α-decay branching ratio of 0.49% could be determined for this isotope. Detailed α–γ coincidence analysis was performed, however only partial α-decay schemes could be constructed for ^{182,184}Tl due to the complexity of the α-decay patterns, limited knowledge on the structure of the daughter nuclei and lack of γ–γ coincidences. The combination of low-lying states in ^{178}Au identified in this work through α–γ coincidences, the laser spectroscopy studies at ISOLDE and the data obtained at a recently performed in-beam study of ^{178}Au at RITU should help to establish the full decay scheme of ^{178}Au. A high-spin and low-spin α-decaying state have already been identified by our latest laser spectroscopy studies at ISOLDE [58]. Reduced α-decay widths or hindrance factors have been calculated for the different α-decay branches in ^{182,184}Tl. From a comparison with values obtained in neighboring odd-A and even-A thallium isotopes, analogies were deduced between states with possibly similar or completely different structures. Only the ^{184}Tl (10^-) state is α decaying unhindered to a state in ^{180}Au, all other α-decay channels observed in this study are hindered, indicating a different underlying structure of the mother and daughter isotopes.

Acknowledgments

We acknowledge the support of the ISOLDE Collaboration and technical teams for providing excellent beams and the GSI Target Laboratory for manufacturing the carbon foils. This work

has been funded by FWO-Vlaanderen (Belgium), by GOA/2010/010 (BOF KU Leuven), by the Interuniversity Attraction Poles Programme initiated by the Belgian Science Policy Office (BriX network P7/12), by the European Commission within the Seventh Framework Programme through I3-ENSAR (contract no RII3-CT-2010–262010), by a grant from the European Research Council (ERC-2011-AdG-291561-HELIOS), by grants from the UK Science and Technology Facilities Council, by the Slovak Research and Development Agency under the contract No APVV-0177-11 and by Slovak grant agency VEGA (contract Nr 2/0121/14).

References

[1] Van Maldeghem J and Heyde K 1990 *Fizika* **22** 233
[2] Heyde K and Wood J L 2011 *Rev. Mod. Phys.* **83** 1467
[3] Coenen E *et al* 1985 *Phys. Rev. Lett.* **54** 1783
[4] Van Duppen P *et al* 1991 *Nucl. Phys.* A **529** 268
[5] Andreyev A N *et al* 2003 *Eur. Phys. J.* A **18** 39
[6] Andreyev A N *et al* 2003 *Eur. Phys. J.* A **18** 55
[7] Kugler E *et al* 2000 *Hyperfine Interact.* **129** 23
[8] Toth K S *et al* 1976 *Phys. Lett.* B **63** 150
[9] Cole J D *et al* 1976 *Abstract Submitted to the Third Int. Conf. on Nuclei far from Stability (Cargese, Corsica)*
[10] Schrewe U J *et al* 1980 *Phys. Lett.* B **91** 46
[11] Ch Böhm *et al* 2014 *Phys. Rev.* C **90** 044307
[12] Van Beveren C *et al* 2015 *Phys. Rev.* C **92** 014325
[13] Keller J G *et al* 1986 *Nucl. Phys.* A **452** 173
[14] Bolshakov V A *et al* 1993 *Proc. 6th Conf. on Nuclei Far from Stability, 9th Int. Conf. on Atomic Masses and Fundamental Constants (Bernkastel-Kues)* p 743
[15] Bouljedri A *et al* 1991 *Z. Phys.* A **339** 311
[16] Batchelder J C *et al* 1997 *Z. Phys.* A **357** 121
[17] Marino L L, Ewbank W B, Shugart H A and Silsbee H B 1958 *Bull. Am. Phys. Soc.* **3** 319
[18] Ekstrom C, Wannberg G and Shishodia Y S 1976 *Hyperfine Interact.* **1** 437
[19] Fuller G H 1976 *J. Phys. Chem. Ref. Data* **5** 835
[20] Menges R *et al* 1992 *Z. Phys.* A **341** 475
[21] Wang M *et al* 2012 *Chin. Phys.* C **36** 1603
[22] Andreyev A N *et al* 2009 *Phys. Rev.* C **80** 054322
[23] Andreyev A N *et al* 2010 *J. Phys. G: Nucl. Part. Phys.* **37** 035102
[24] Carpenter M P *et al* 2005 *J. Phys. G: Nucl. Part. Phys.* **31** S1599
[25] Evaluated Nuclear Structure Data File (ENSDF) 2015 (http://nndc.bnl.gov.com)
[26] Elseviers J *et al* 2011 *Phys. Rev.* C **84** 034307
[27] Barzakh A E *et al* 2015 in preparation
[28] Fedoseev V N *et al* 2000 *Hyperfine Interact.* **127** 409
[29] Fedoseev V N *et al* 2012 *Rev. Sci. Instrum.* **83** 02A903
[30] Fedoseev V N, Kudryavtsev Yu and Mishin V I 2012 *Phys. Scr.* **85** 058104
[31] Alkhazov G D *et al* 1992 *Nucl. Instr. Meth.* B **69** 517
[32] Barzakh A E *et al* 1998 *Eur. Phys. J.* A **1** 3
[33] Fedoseev V N *et al* 2003 *Nucl. Instr. Meth.* B **204** 353
[34] Andreyev A N *et al* 2010 *Phys. Rev . Lett.* **105** 252502
[35] Elseviers J *et al* 2013 *Phys. Rev.* C **88** 044321
[36] Seliverstov M *et al* 2014 *Phys. Rev.* C **89** 034323
[37] Rapisarda E *et al* 2015 in preparation
[38] Lommel B *et al* 2002 *Nucl. Instr. Meth.* A **480** 199
[39] X ray instruments Associates 2010 (www.xia.com)
[40] Wauters J *et al* 1994 *Phys. Rev.* C **50** 2768
[41] Bingham C R *et al* 1995 *Phys. Rev.* C **51** 125
[42] Wauters J *et al* 1993 *Z. Phys.* A **345** 21
[43] Cocolios T E *et al* 2010 *J. Phys. G: Nucl. Part. Phys.* **37** 125103
[44] Andreyev A N *et al* 1999 *Eur. Phys. J.* A **6** 381

[45] Hessberger F P *et al* 1989 *Nucl. Instr. Meth.* A **274** 522
[46] Rasmussen J O *et al* 1959 *Phys. Rev.* **113** 1593
[47] Hansen P G *et al* 1970 *Nucl. Phys.* A **148** 249
[48] Hagberg E *et al* 1979 *Nucl. Phys.* A **318** 29
[49] Rytz A 1991 *At. Data Nucl. Data Tables* **47** 205
[50] Andreyev A E, Huyse M and Van Duppen P 2013 *Rev. Mod. Phys.* **85** 1541
[51] Ghys L *et al* 2015 *Phys. Rev.* C **91** 044314
[52] Raddon P M *et al* 2004 *Phys. Rev.* C **70** 064308
[53] Andreyev A N *et al* 2006 *Phys. Rev.* C **73** 044324
[54] Liberati V *et al* 2013 *Phys. Rev.* C **88** 044322
[55] Toth K S *et al* 1998 *Phys. Rev.* C **58** 1310
[56] Kondev F G *et al* 2013 *EPJ Web of Conferences* **63** 01013
[57] Andreyev A N 2015 private communication
[58] Whitmore B 2014 Decay spectroscopy of 178Au *Master's Thesis* University of York